Iranian Journal of Medical Physics

ijmp.mums.ac.ir

Mass Attenuation Coefficients of Human Body Organs using MCNPX Monte Carlo Code

Huseyin Ozan Tekin[1,4*], Viswanath P. Singh[2], Elif Ebru Altunsoy[3,4], Tugba Manici [4],

Mohammed I. Sayyed[5]

[1] Department of Radiotherapy, Vocational School of Health Services, Uskudar University, Istanbul 34672, Turkey
[2] Department of Physics, Faculty of Science, Karnatak University, Dharwad, 580003, India
[3] Department of Medical Imaging, Vocational School of Health Services, Uskudar University, İstanbul 34672, Turkey
[4] Medical Radiation Research Center (USMERA), Uskudar University, Istanbul 34672, Turkey
[5] Department of Physics, Faculty of Science, University of Tabuk, Tabuk, KSA

ARTICLE INFO

Article type:
Original Article

Article history:
Received: May 16, 2017
Accepted: Jun 04, 2017

Keywords:
Attenuation Coefficient
Monte Carlo
MCNP-X

ABSTRACT

Introduction: Investigation of radiation interaction with living organs has always been a thrust area in medical and radiation physics. The investigated results are being used in medical physics for developing improved and sensitive techniques and minimizing radiation exposure. In this study, mass attenuation coefficients of different human organs and biological materials such as adipose, blood, bone, brain, eye lens, lung, muscle, skin, and tissue have been calculated.

Materials and Methods: In the present study, Monte Carlo N-Particle eXtended (MCNP-X) version 2.4.0 was used for determining mass attenuation coefficients, and the obtained results were compared with earlier investigations (using GEometry ANd Tracking [GEANT4] and FLUKA computer simulation packages) for blood, bone, lung, eye lens, adipose, tissue, muscle, brain, and skin materials at different energies.

Results: The results of this study showed that the obtained results from MCNP-X were in high accordance with the National Institute of Standards and Technology data.

Conclusion: Our findings would be beneficial for use of present simulation technique and mass attenuation coefficients for medical and radiation physics applications.

► *Please cite this article as:*
Tekin HO, Singh VP, Altunsoy EE, Manici T, Sayyed M. Mass Attenuation Coefficients of Human Body Organs using MCNPX Monte Carlo Code. Iran J Med Phys 2017; 14: 229-240. 10.22038/ijmp.2017.23478.1230.

Introduction

Experimental investigation on living organs is not always possible; therefore, theoretical and simulation investigations play a pivotal role in the area of radiation and medical physics. Constant improvement in medical physics and exposure reduction has been witnessed in the treatment of various types of diseases using radiation therapy. Special care is required for radiation therapy to avoid undue exposure of normal human organs. Medical imaging is the process of creating visual representations of the interior of a body for analysis and treatment.

Image formation is dependent upon interaction of radiation (scattering and absorption) with body parts. Medical images are formed due to differences in interaction properties. Medical imaging is being used in positron emission tomography (PET) and computed tomography (CT) scan for scanning various body parts. Increased resolution of images is one of the crucial requirements of a medical physicist. The contrast of the medical image depends upon photon attenuation in the sample. For monochromatic photon beams, the intensity decreases as the photon beam propagates through the sample or human body organ according to the Lambert-Beer law [$I=I_0 \exp(-\mu t)$], where I_0 is the incident intensity, t is the path length, and μ is the sample's linear attenuation coefficient. This coefficient depends on elemental or chemical composition of the sample and is larger for electron-dense materials. Therefore, materials such as metal, bone, and kidney stones have high image contrast against soft tissues [1].

As the linear attenuation coefficient of a material is at play in image formation, measurement of the linear attenuation coefficients of human body parts is mandatory. The linear attenuation coefficient (cm^{-1}) provides information concerning the fraction of photons removed from a mono-energetic beam of gamma ray per unit volume of material. Photon interaction probability varies with material density; therefore, the linear attenuation coefficients are material dependent. To overcome this drawback,

*Corresponding Author: Department of Radiotherapy, Vocational School of Health Services, Uskudar University, Istanbul 34672, Turkey. Tel: +905455018843, E-mail: huseyinozan.tekin@uskudar.edu.tr

mass attenuation coefficient (cm^2/g) was introduced, which is calculated by linear attenuation coefficient divided by density. The mass attenuation coefficient is a fundamental photon interaction property for calculation of effective atomic number, effective electron density, and shielding properties in materials or human organs [2]. The attenuation coefficients of various types of biological materials (normal and cancerous tissues) [3-5], human body organs [6], tissue substitutes [7-9], and dosimeters [2] were investigated by different researchers. Neutron interaction of human body organs and shielding materials was also reported in a number of studies [10].

The X, gamma, and neutron interaction parameters of human body organs were investigated by theoretical, simulation, and experimental studies. The theoretical investigation is possible by XCOM software [11] and simulation by Monte Carlo methods. Experimental investigation in the field of radiation and medical physics is cumbersome due to unavailability of sample materials; therefore, most of the investigations were carried out on human body organ phantoms or simulations of the original samples in computer environment, and the obtained results were compared with those registered at standard databases. Presently, Monte Carlo simulation method is being used by GEometry ANd Tracking (GEANT4) and FLUKA [12, 13]. Monte Carlo N-Particle Transport Code System-eXtendend (MCNP-X) for multi-particle and high-energy applications is another simulation method [14].

Some investigations are found for mass attenuation coefficients using Monte Carlo simulation [15-18]. Various simulation investigations by using MCNP-X Monte Carlo code are found in the literature. Availability of MCNP-X on detection efficiency and use of various experimental and Monte Carlo studies were investigated by Akkurt et al. [19]. In addition, conditions of MCNP-X for dose distribution and attenuation properties at the nanoscale were studied by Tekin et al. [20-24]. Development and validation of treatment plan verification system based on MCNP-X were studied by Jabbari and Monadi [25].

To the best of our knowledge, no study has used MCNP-X simulation of mass attenuation coefficients of human body organs. This has encouraged us to investigate the attenuation properties of human organs and compare them with the previous findings. Radiation interaction parameters obtained by theoretical, simulation and experimental studies are expected to be the same. Therefore, comparison of results using different methods is a useful validation technique.

Materials and Methods

In the present study, MCNP-X (Los Alamos National Laboratory, U.S.A) was used for determining mass attenuation coefficients and compared with earlier investigations using GEANT4 (CERN-Switzerland and other high energy physics labs worldwide) and FLUKA (INFN-Italy and CERN-Switzerland) simulations for blood, bone, lung, eye lens, adipose, tissue, muscle, brain, and skin materials at different energies. The acquired results were compared with XCOM and National Institute of Standards and Technology (NIST) standard databases. In the present investigation, the standardized MCNP-X simulation geometry was employed [18]. The present investigation would be very useful for further utilization of standardized MCNP-X simulation method for low atomic number materials and medical applications. Due to wide applications of MCNP-X in medical and radiation attenuation investigations, this comparative study can create a database on mass attenuation coefficients. The elemental concentrations and densities (d) of the samples [26] are presented in Table 1. In this study, MCNP-X (version 2.4.0, Monte Carlo N–Particle Transport Code System) was used for exploring attenuation properties of human body organs.

MCNP-X is a radiation transport code for modelling the interaction of radiation with materials and tracks all particles at different energies. MCNP-X is fully three-dimensional and utilizes extended nuclear cross section libraries and physics models for particle types. MCNP-X is a significantly convenient tool for attenuation and energy deposition investigations. MCNP-X simulation parameters such as cell, surface, and material definitions, position of each tool, as well as definitions and features of sources are defined in input file according to their properties.

As one of the main rules of photon-matter interaction, photon loses energy as it passes through matter by some physical processes such as photoelectric effect, Compton scattering, and pair production. The geometrical forms have been defined as a cube with the sizes of 10 cm (height) x 10 cm (width) x 5 cm (thickness). The total simulation geometry is outlined in Figure 1. The schematic view of MCNP-X simulation setup with lead (Pb) collimator, investigated organ sample, Pb shields for backscattered photons, and detection area with defined geometries in MCNP-X input file are presented in Figure 2. Gamma-ray source, Pb (density=11.34 g/cm^3) collimators and shields, samples and detection area have been defined in cell card, surface card, and data card sections of MCNP-X input by considering different variables such as CEL, ERG, DIR, POS, and PAR.

Table 1. Elemental weight (%) concentrations of the investigated organs

Elemental concentration (%)	Adipose tissue (d=0.92 g/cm³	Blood (d=1.069 g/cm³	Bone (d=1.85 g/cm³	Brain (d=1.039 g/cm³	Eye Lens (d=1.1 g/cm³	Lung (d=1.05 g/cm³	Muscle (d=1.04 g/cm³	Skin (d=1.1 g/cm³	Tissue (d=1.00 g/cm³
H	0.11947	0.10186	0.06398	0.11066	0.09926	0.10127	0.10063	0.10058	0.10447
C	0.63724	0.10002	0.27800	0.12542	0.19371	0.10231	0.10783	0.22825	0.23219
N	0.00797	0.02964	0.02700	0.01328	0.05327	0.02865	0.02768	0.04642	0.02488
O	0.23233	0.75941	0.41001	0.73772	0.65375	0.75707	0.75477	0.61900	0.63023
Nn	0.00050	0.00185	-	0.00184	-	0.00184	0.00075	0.00007	0.00113
Mg	0.00002	0.00004	0.00200	0.00015	-	0.00073	0.00019	0.00006	0.00013
Si	-	0.00003	-	-	-	-	-	-	-
P	-	0.00035	0.07000	0.00354	-	0.00080	0.00180	0.00033	0.00133
S	0.00016	0.00185	0.00200	0.00177	-	0.00225	0.00241	0.00159	0.00199
Cl	0.00119	0.00278	-	0.00236	-	0.00266	-	0.00267	0.00134
K	-	0.00163	-	0.00310	-	0.00194	-	0.00085	0.00199
Ca	-	0.00006	0.14700	0.00009	-	0.00009	-	0.00015	0.00023
Fe	-	0.00045	-	0.00005	-	0.00037	-	0.00001	0.00005
Zn	-	0.00001	-	0.00001	-	0.00001	-	0.00001	0.00003

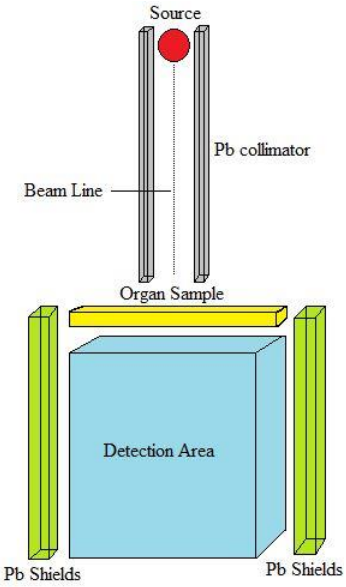

Figure 1. Total simulation geometry

The geometric center of the detection area has been considered for the location of a point source. The source has been defined in the mode card as a point source at photon energies of 60, 80, 150, 400, 500, 600, 1000, 1250, 1500, and 2000 keV. To acquire absorbed dose amounts in the detection area, average flux tally F4 is employed. This type of tally in MCNP-X scores average flux in a point or cell.

On the other hand, 10^8 particles have been tracked as the number of particles (NPS variable). MCNP-X calculations were completed by using Intel® Core ™ i7 CPU 2.80 GHz computer hardware.

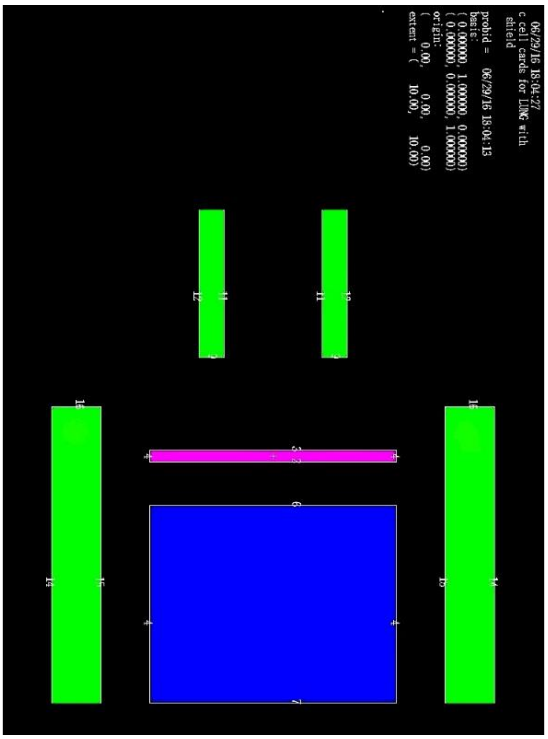

Figure 2. MCNP-X simulation setup of total simulation geometry

During the simulation study, the error rate is observed to be less than 1% of the output file. The expected particle counting for the simulation output data is selected as a photon (PAR=2). This type of approach is an important variance reduction method for diminishing statistical error and optimizing the computer processor by ignoring the unused particle counting for the output data. The same simulation parameters are applied for all organ samples. A detection system built on the Monte Carlo simulation code does not work as an experimental scintillation detector does, which explains the slight differences in the calculation process. A detection system is based on finding a result from the analysis of changes in the graph, which gives the transmitted radiation dose depending on the attenuator thickness. Since MCNP-X has the ability to calculate average flux in a cell, we performed mass attenuation calculations for each given energy value. By applying the mentioned calculation process into Lambert-Beer law, we calculated each investigated organ's mass attenuation coefficients. This study focused on comparative investigation of three well-known Monte Carlo codes including MCNP-X, FLUKA, and GEANT4.

Results

The calculated mass attenuation coefficients of human body organs by using MCNP-X Monte Carlo code and the comparison with available data in the literature [22] are tabulated in tables 2-10 and presented in figures 3-11, respectively. To analyse and compare standard deviation rates between standard NIST data and Monte Carlo programs, we calculated the deviations between NIST data and Monte Carlo results (tables 11-13). The deviation rates were calculated by using the formula of ($D=E_a-E_b/E_b\times100\%$). In this formula, E_a is the first result and E_b is the second result in calculating the standard deviation of two values.

Table 2. Calculated mass attenuation coefficients for adipose (d=0.92 g/cm^3)

Energy (kev)	MCNPX	FLUKA	GEANT4	XCOM	NIST
60	0,1976	0,19806	0,18615	0,1974	0,1974
80	0,1802	0,17985	0,17707	0,1805	0,18
150	0,1534	0,15058	0,14824	0,1506	0,15
400	0,1065	0,10653	0,10641	0,1067	0,1062
500	0,0977	0,09881	0,09742	0,0974	0,09696
600	0,0901	0,08951	0,08951	0,09009	0,08965
1000	0,0722	0,0706	0,07279	0,07113	0,07078
1250	0,0674	0,06332	0,06329	0,06361	0,0633
1500	0,0593	0,05778	0,05763	0,05789	0,0576
2000	0,0508	0,05016	0,04979	0,04964	0,0494

Table 3. Calculated mass attenuation coefficients for blood (d=1.069 g/cm^3)

Energy (kev)	MCNPX	FLUKA	GEANT4	XCOM	NIST
60	0,2068	0,2033	0,19302	0,205	0,2057
80	0,1862	0,18345	0,17421	0,1824	0,1827
150	0,1443	0,14866	0,14603	0,1492	0,1492
400	0,1054	0,10593	0,10402	0,1052	0,1052
500	0,0962	0,09453	0,09592	0,09598	0,09598
600	0,0886	0,08956	0,08845	0,08873	0,08874
1000	0,0703	0,07088	0,0705	0,07006	0,07007
1250	0,0626	0,06252	0,06226	0,06265	0,06265
1500	0,0571	0,05751	0,05678	0,05701	0,05701
2000	0,0484	0,0487	0,04876	0,04896	0,04896

Table 4. Calculated mass attenuation coefficients for bone (d=1.85 g/cm^3)

Energy (kev)	MCNPX	FLUKA	GEANT4	XCOM	NIST
60	0,2761	0,27581	0,2533	0,2752	0,3148
80	0,2081	0,20855	0,19483	0,2087	0,2229
150	0,1498	0,14942	0,14325	0,1491	0,148
400	0,1022	0,10136	0,09948	0,1018	0,0991
500	0,0929	0,09263	0,09333	0,09275	0,09022
600	0,0859	0,08547	0,08548	0,0856	0,08332
1000	0,0684	0,06738	0,06759	0,06758	0,06566
1250	0,0609	0,06061	0,06013	0,06043	0,05871
1500	0,0561	0,05478	0,05556	0,05501	0,05346
2000	0,0484	0,0471	0,04737	0,04733	0,04607

Table 5. Calculated mass attenuation coefficients for brain (d=1.039 g/cm^3)

Energy (keV)	MCNPX	FLUKA	GEANT4	XCOM	NIST
60	0,2072	0,20274	0,19398	0,2065	0,2058
80	0,1844	0,18351	0,17661	0,1838	0,1831
150	0,1516	0,14752	0,1469	0,1503	0,1498
400	0,1064	0,10443	0,10563	0,106	0,1056
500	0,0993	0,09456	0,09716	0,09672	0,0964
600	0,0921	0,08729	0,09047	0,08942	0,08913
1000	0,0722	0,06932	0,07082	0,07061	0,07037
1250	0,0648	0,06163	0,06321	0,06314	0,06293
1500	0,0583	0,05671	0,0579	0,05745	0,05726
2000	0,0498	0,04799	0,04893	0,04933	0,04917

Table 6. Calculated mass attenuation coefficients for eye lens (d=1.1 g/cm^3)

Energy (keV)	MCNPX	FLUKA	GEANT4	XCOM	NIST
60	0,2032	0,20135	0,18781	0,2007	0,2013
80	0,1833	0,18078	0,17071	0,1803	0,1803
150	0,1496	0,14807	0,14558	0,1486	0,1482
400	0,1045	0,10482	0,10367	0,1049	0,1046
500	0,0968	0,09683	0,09603	0,09576	0,09547
600	0,0896	0,08854	0,09041	0,08853	0,08827
1000	0,0702	0,06961	0,07035	0,06991	0,06969
1250	0,0624	0,06138	0,06274	0,06251	0,06232
1500	0,0569	0,05615	0,05699	0,05688	0,05671
2000	0,0489	0,04869	0,04795	0,04884	0,04869

Table 7. Calculated mass attenuation coefficients for lung (d=1.05 g/cm^3)

Energy (keV)	MCNPX	FLUKA	GEANT4	XCOM	NIST
60	0,2042	0,20323	0,18919	0,2052	0,2053
80	0,1823	0,1838	0,17419	0,1824	0,1826
150	0,1487	0,14833	0,14702	0,1491	0,1493
400	0,1046	0,10461	0,10382	0,1051	0,1053
500	0,0968	0,09585	0,09596	0,09592	0,09607
600	0,0896	0,08911	0,08915	0,08869	0,08882
1000	0,0704	0,07071	0,07006	0,07002	0,07013
1250	0,0627	0,06182	0,06199	0,06262	0,06271
1500	0,0575	0,05684	0,05649	0,05698	0,05706
2000	0,0497	0,04909	0,04831	0,04893	0,049

Table 8. Calculated mass attenuation coefficients for muscle (d=1.04 g/cm^3)

Energy (keV)	MCNPX	FLUKA	GEANT4	XCOM	NIST
60	0,2051	0,20207	0,19035	0,2033	0,2048
80	0,1836	0,18323	0,17421	0,1816	0,1823
150	0,1498	0,14823	0,14527	0,149	0,1492
400	0,1063	0,1055	0,10434	0,1051	0,1052
500	0,0964	0,09622	0,09588	0,09592	0,09598
600	0,0894	0,08842	0,08939	0,08868	0,08874
1000	0,0702	0,07003	0,06998	0,07002	0,07007
1250	0,0632	0,06351	0,0618	0,06261	0,06265
1500	0,0572	0,05635	0,05668	0,05698	0,05701
2000	0,0487	0,0478	0,0471	0,04893	0,04896

Table 9. Calculated mass attenuation coefficients for skin (d=1.1 g/cm^3)

Energy (keV)	MCNPX	FLUKA	GEANT4	XCOM	NIST
60	0,2021	0,20108	0,18962	0,2019	-
80	0,1811	0,18023	0,17506	0,1809	-
150	0,1493	0,14921	0,1459	0,1488	-
400	0,1041	0,10489	0,10445	0,105	-
500	0,0961	0,09693	0,09548	0,09586	-
600	0,0894	0,08669	0,08815	0,08863	-
1000	0,0704	0,07069	0,06908	0,06998	-
1250	0,0629	0,06252	0,06361	0,06257	-
1500	0,0571	0,0572	0,05682	0,05694	-
2000	0,0491	0,04868	0,0487	0,04888	-

Table 10. Calculated mass attenuation coefficients for tissue (d=1.00 g/cm^3)

Energy (keV)	MCNPX	FLUKA	GEANT4	XCOM	NIST
60	0,2019	0,20167	0,19044	0,2033	0,2048
80	0,1841	0,18317	0,17369	0,1817	0,1823
150	0,1496	0,14863	0,14492	0,1493	0,1492
400	0,1049	0,10446	0,10591	0,1054	0,1052
500	0,0954	0,09524	0,09592	0,09619	0,09598
600	0,0889	0,08882	0,08923	0,08893	0,08873
1000	0,0701	0,06922	0,07041	0,07022	0,07006
1250	0,0629	0,06294	0,06226	0,06279	0,06265
1500	0,0572	0,05801	0,05674	0,05714	0,05701
2000	0,0491	0,04866	0,04915	0,04905	0,04895

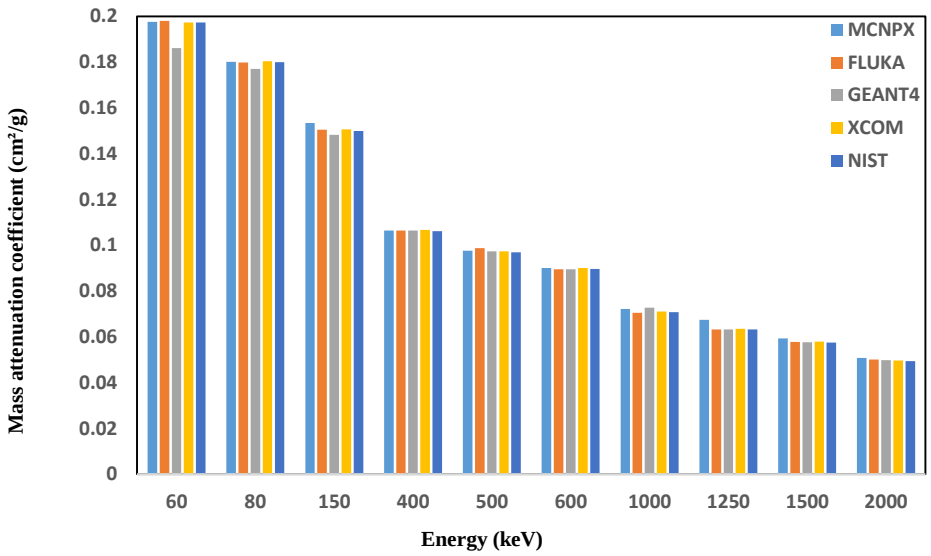

Figure 3. Mass attenuation coefficients for adipose tissue

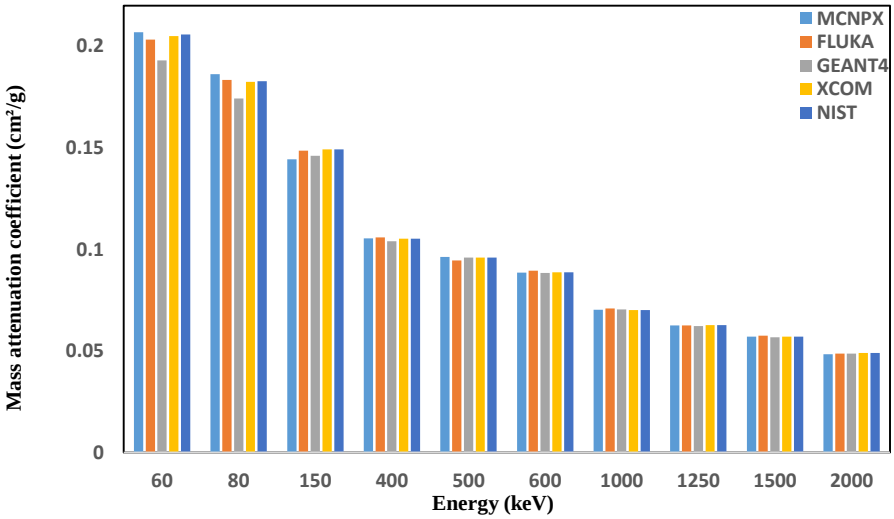

Figure 4. Mass attenuation coefficients for blood

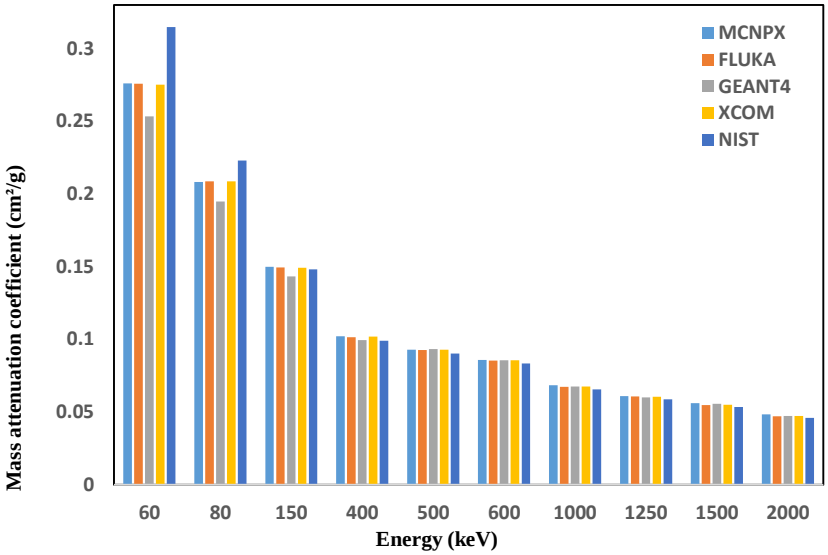

Figure 5. Mass attenuation coefficients for bone

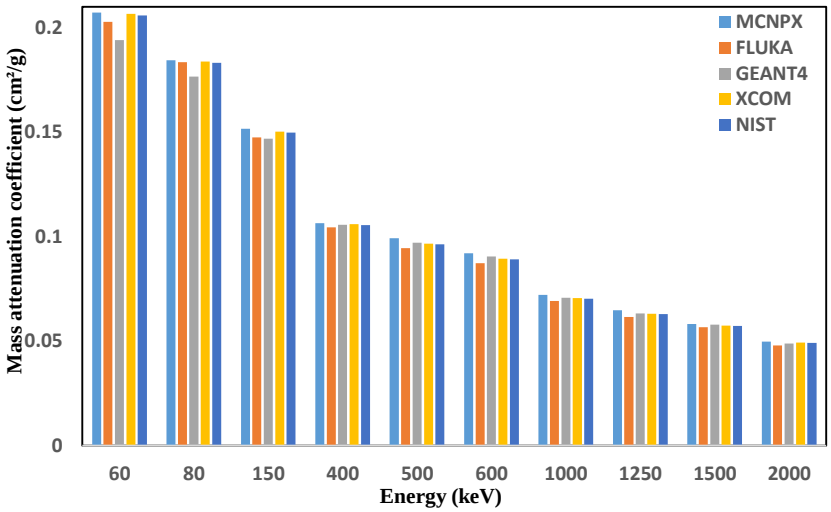

Figure 6. Mass attenuation coefficients for brain

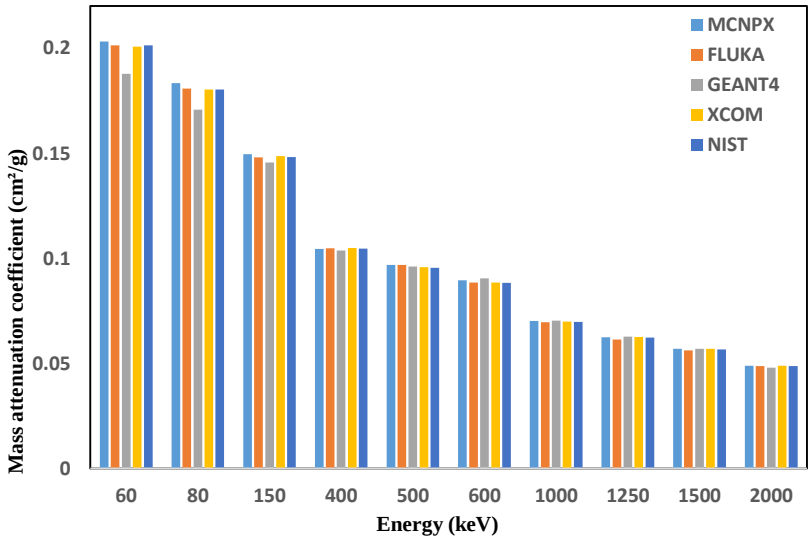

Figure 7. Mass attenuation coefficients for eye lens

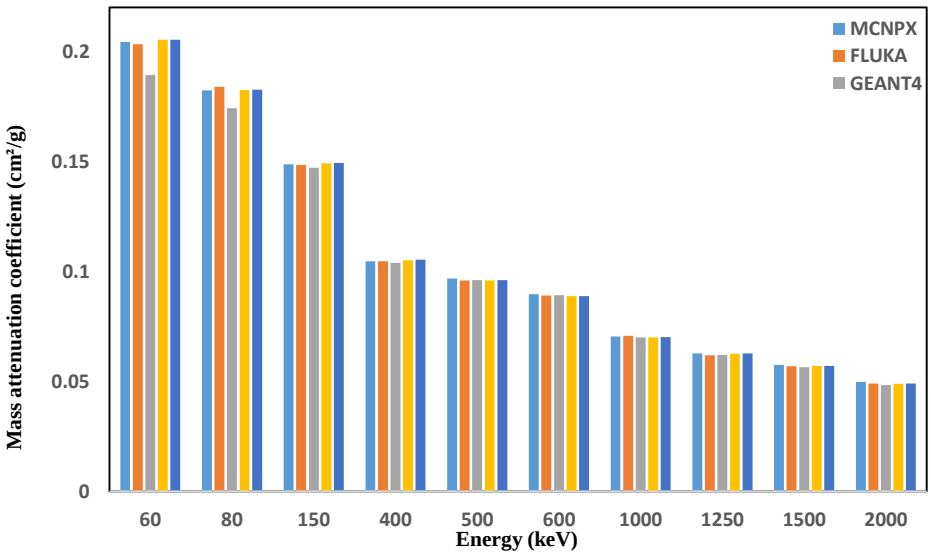

Figure 8. Mass attenuation coefficients for lung

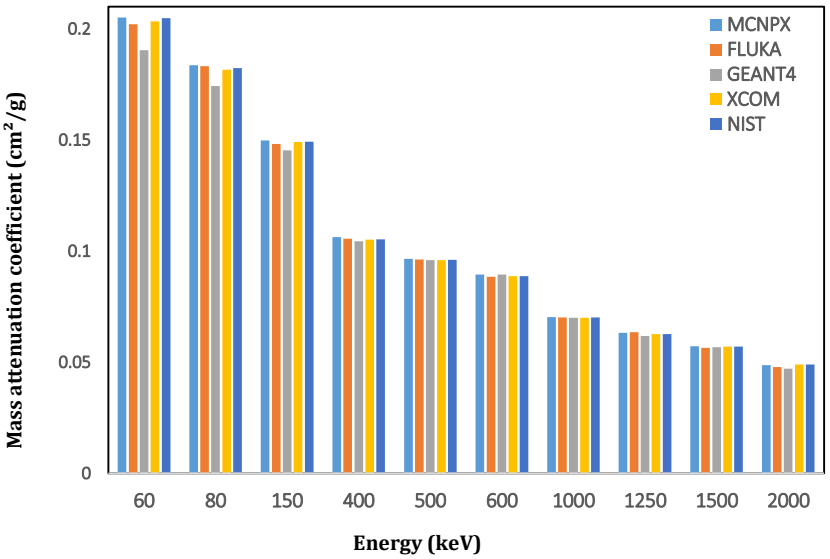

Figure 9. Mass attenuation coefficients for eye muscle

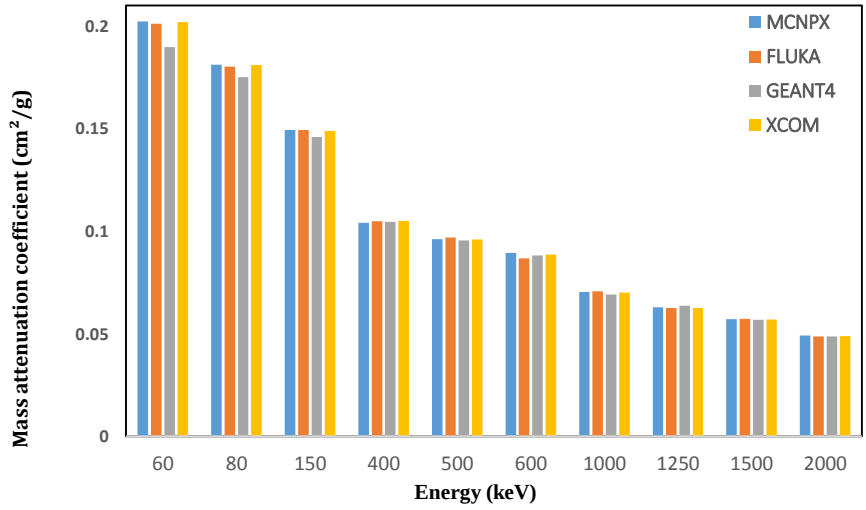

Figure 10. Mass attenuation coefficients for skin

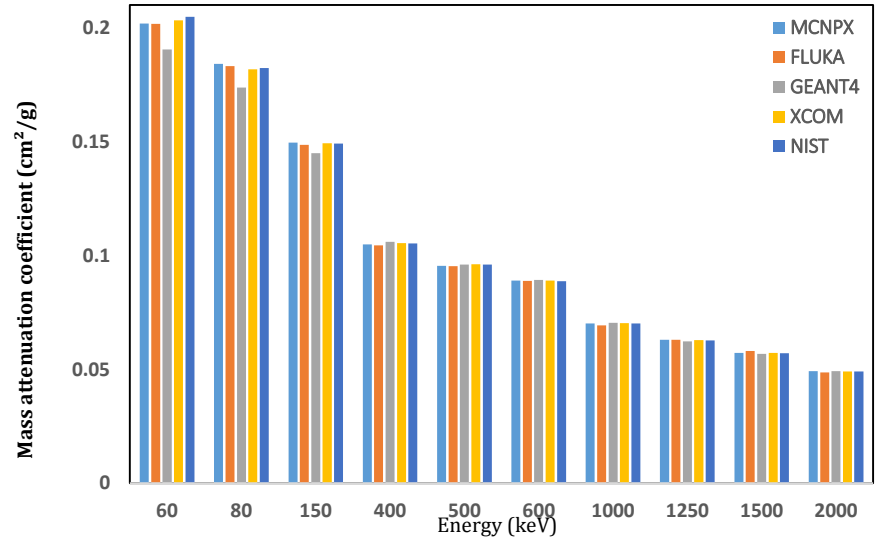

Figure 11. Mass attenuation coefficients for tissue

Table 11. Calculated standard deviations between standard NIST data and MCNPX (%)
($D=E_a-E_b/E_b\times 100\%$)

	60 keV	80 keV	150 keV	400 keV	500 keV	600 keV	1000 keV	1250 keV	1500 keV	2000 keV
AdiposeTissue	0,1012	0,1109	2,2164	0,2116	0,7574	0,4994	1,9667	6,083	2,8667	2,7559
Blood	0,5319	1,8796	3,3957	0,1897	0,2286	0,158	0,3271	0,0798	0,1576	0,157
Bone	14,0166	7,1119	1,2016	3,0332	2,8848	3,0034	4,0058	3,596	4,7058	4,814
Brain	0,6756	0,7049	1,1873	0,7518	2,9204	3,2247	2,5346	2,8858	1,7838	1,265
Eye Lens	0,935	1,6366	0,9358	0,0956	1,3739	1,4843	0,7264	0,1282	0,3339	0,4294
Lung	0,5386	0,1645	0,4034	0,6692	0,7541	0,8705	0,3835	0,0159	0,7652	1,4084
Muscle	0,1462	0,708	0,4005	1,0348	0,4356	0,7382	0,1851	0,8702	0,3321	0,5338
Skin	-	-	-	-	-	-	-	-	-	-
Tissue	1,4363	0,9777	0,2673	0,2859	0,6079	0,1912	0,057	0,3974	0,3321	0,3054

Table 12. Calculated standard deviations between standard NIST data and FLUKA (%)
($D=E_a-E_b/E_b\times 100\%$)

	60 keV	80 keV	150 keV	400 keV	500 keV	600 keV	1000 keV	1250 keV	1500 keV	2000 keV
AdiposeTissue	0,3332	0,0834	0,3851	0,3097	1,8722	0,1564	0,2549	0,0315	0,3115	1,5151
Blood	1,1805	0,4088	0,3632	0,6891	1,5339	0,9155	1,1427	0,2079	0,8694	0,5338
Bone	14,1365	6,8808	0,9503	2,2296	2,6017	2,5155	2,5526	3,1347	2,4096	2,1868
Brain	1,5093	0,2234	1,5455	1,1203	1,9458	2,1079	1,5147	2,1093	0,9698	2,4588
Eye Lens	0,0248	0,2655	0,0877	0,2098	1,4045	0,3049	0,1149	1,5314	0,9973	0
Lung	1,0185	0,6528	0,6539	0,6595	0,2295	0,3254	0,8202	1,4396	0,387	0,1833
Muscle	1,351	0,5075	0,6543	0,2843	0,2494	0,3619	0,0571	1,3541	1,1712	2,4267
Skin	-	-	-	-	-	-	-	-	-	-
Tissue	1,552	0,4749	0,3835	0,7084	0,7769	0,1013	1,2135	0,4607	1,7238	0,5959

Table 13. Calculated standard deviations between standard NIST data and GEANT4 (%)
($D=E_a-E_b/E_b\times 100\%$)

	60 keV	80 keV	150 keV	400 keV	500 keV	600 keV	1000 keV	1250 keV	1500 keV	2000 keV
Adipose Tissue	6,0435	1,6547	1,1872	0,1973	0,4721	0,1564	2,7613	0,0158	0,052	0,7832
Blood	6,5692	4,8734	2,1707	1,1343	0,0625	0,3278	0,6099	0,6264	0,405	0,4101
Bone	24,2795	14,4074	3,3158	0,3819	3,3322	2,5269	2,8554	2,3615	3,7796	2,7444
Brain	6,0934	3,6747	1,9741	0,0284	0,7822	1,4811	0,6354	0,4429	1,1053	0,4904
Eye Lens	7,1827	5,6177	1,7996	0,897	0,5831	2,3669	0,9381	0,6694	0,4913	1,5432
Lung	1,5816	1,2881	0,3486	0,2243	0,0479	0,1014	0,0085	0,05	0,1472	0,3763
Muscle	7,5912	4,6438	2,7053	0,8242	0,1042	0,7271	0,1286	1,3754	0,5822	3,949
Skin	-	-	-	-	-	-	-	-	-	-
Tissue	7,5404	4,9571	2,9533	0,6703	0,0625	0,5603	0,497	0,6264	0,4758	0,4069

Discussion

Standard deviation values were calculated for each simulation code separately. As observed in tables 11-13, FLUKA and MCNP-X had almost similar deviations for the investigated organs. It can be concluded that each Monte Carlo code has different abilities in different energy regions. In the low-energy area, standard deviation rates of MCNP-X and FLUKA were less than those of GEANT4. It can be clearly noted in Table 13 that the highest standard deviation rates were obtained for GEANT4 data. The mass attenuation coefficients of all the human body organs were found the low for GEANT4 in low-energy region (up to 150 keV).

Our standard deviation calculations showed that GEANT4 results visibly increased at energies above 400 keV. This could be due to the fact that GEANT4 is designed for high-energy applications. However, MCNP-X, FLUKA, GEANT4, NIST, and XCOM results of mass attenuation coefficients were in good agreement at photon energies above 150 keV. It was observed that photon attenuation parameter of each sample decreased with enhanced photon energy due to more penetration of the photons from the attenuator. In low-energy regions (up to 500 keV), MCNP-X results were slightly more compatible with those of FLUKA and GEANT4, when compared to the standard NIST values. This result indicates that MCNP-X may be a more suitable program for live

biological media investigations at low-energy regions since it has extensive cross section library for low-energy regions. The results also reflected that use of MCNP-X in wide energy regions might need separate calculations of low-, medium-, and high-energy contributions, which can be referred to as the major disadvantage of MCNP-X code.

This study allowed comparison of three well-known Monte Carlo codes. The mass attenuation coefficients of human body organs were found comparable with theoretical and standard NIST results. The MCNP-X simulation was also found comparable with GEANT4 and FLUKA, and so were their simulated mass attenuation coefficients.

Conclusion

In this study, the obtained data from Monte Carlo for mass attenuation coefficients as a function of incoming photon energy was presented. The mass attenuation coefficients of human body organs were investigated using MCNP-X for photon energy range of 60-2000 keV with standard simulation geometry. The standard deviation of mass attenuation coefficients simulated by MCNP-X and NIST data were found very small, indicating that the results of the present investigation were in very good agreement with the standard database, while a slightly higher standard deviation was observed for bone. The discrepancy between some results could be due to differences between cross-section libraries of Monte Carlo programs. This study proved that MCNP-X code is a suitable and efficient code for mass attenuation coefficients in low- and high-energy fields and can be beneficial for future studies, where experimental conditions and data are not available. Standard simulation geometry and mass attenuation coefficients can be utilized for medical and radiation physics applications. It can be also concluded that calculated mass attenuation properties of various human organs can be very useful as a standard data for calculation of absorbed dose values in CT scan and other medical radiation studies.

References

1. Hongyu Chen, Melissa M. Rogalski, Jeffrey N. Anker. Advances in functional X-ray imaging techniques and contrast agents. Phys Chem Chem Phys. 2012 October 21; 14(39): 13469–86. DOI: 10.1039/C2CP41858D.
2. V. P. Singh, N. M. Badiger. Photon interaction properties of some semiconductor detectors. Nuclear Reactor Technology. 2016; 27: 72 . DOI:10.1007/s41365-016-0076-8.
3. V. P. Singh, N. M. Badiger. Energy absorption buildup factors. effective atomic numbers and air-kerma for human body parts, vitamins and tissue substitutes. J. Radioanalytical and Nuclear Chemistry.2015; 303 (3): 1983-90 .
4. S. Mirji, N. M.badiger, S. S. Kulkarni, M. K. Tiwari. Measurement of linear attenuation coefficients of normal and malignant breast tissues using synchrotron radiation. X-Ray Spectrometry. 2016 May 1;45(3):185-9.. DOI: 10.1002/xrs.2685.
5. Tomal A, Mazarro I, Kakuno EM, Poletti ME. Experimental determination of linear attenuation coefficient of normal, benign and malignant breast tissues. Radiat. Meas. 2010; 45: 1055–9 . DOI:10.1016/j.radmeas.2010.08.008.
6. M. L.Taylor. Quantification of differences in the effective atomic numbers of healthy and cancerous tissues: a discussion in the context of diagnostics and dosimetry. Med Phys. 2012 Sep;39(9):5437-45. DOI: 10.1118/1.4742849.
7. Singh VP, Badiger NM, Kucuk N. Assessment of methods for estimation of effective atomic numbers of common human organ and tissue substitutes: waxes, plastics and polymers. Radioprotection. 2014 Apr;49(2):115-21. DOI: 10.1051/radiopro/2013090.
8. Singh VP, Badiger NM. Study of effective atomic numbers and electron densities, kerma of alcohols, phantom and human organs, and tissues substitutes. Nuclear Technology and Radiation Protection. 2013;28(2):137-45.
9. Singh VP, Badiger NM. Effective atomic numbers of some tissue substitutes by different methods: a comparative study. Journal of Medical Physics/Association of Medical Physicists of India. 2014 Jan;39(1):24. DOI: 10.4103/0971-6203.125489.
10. Singh VP, Badiger NM, Vega-Carrillo RH. Studies on neutron and photon kerma parameters for human body organs. Nuclear Technology and Radiation Protection. 2016;31(2):128-34. DOI: 10.2298/NTRP1602128S.
11. Berger MJ, Hubbell JH. Photon Cross section on a Personal Computer (XCOM). Center for Radiation Research of Standards, MD. 1987;20899.
12. Agostinelli S, Allison J, Amako KA, Apostolakis J, Araujo H, Arce P, Asai M, Axen D, Banerjee S, Barrand G, Behner F. GEANT4—a simulation toolkit. Nuclear instruments and methods in physics research section A: Accelerators, Spectrometers, Detectors and Associated Equipment. 2003 Jul 1;506(3):250-303.
13. Allison J, Amako K, Apostolakis J, Araujo HA, Dubois PA, Asai MA, Barrand GA, Capra RA, Chauvie SA, Chytracek RA, Cirrone GA. Geant4 developments and applications. IEEE Transactions on Nuclear Science. 2006 Feb;53(1):270-8. DOI: 10.1109/TNS.2006.869826.
14. RSICC Computer Code Collection. MCNP-X User's manual Version 2.4.0. Monte Carlo N-Particle Transport Code System for Multiple and High Energy Applications. 2002.
15. Singh VP, Shirmardi SP, Medhat ME, Badiger NM. Determination of mass attenuation coefficient for some polymers using Monte Carlo simulation. Vacuum. 2015 Sep 30; 119: 284-8. DOI: 10.1016/j.vacuum.2015.06.006.
16. El-Khayatt AM, Ali AM, Singh VP, Badiger NM. Determination of mass attenuation coefficient of low-Z dosimetric materials. Radiation Effects and

Defects in Solids. 2014 Dec 2; 169(12): 1038-44. DOI: 10.1080/10420150.2014.988626.
17. Akar A, Baltaş H, Çevik U, Korkmaz F, Okumuşoğlu NT. Measurement of attenuation coefficients for bone, muscle, fat and water at 140, 364 and 662 keV c-ray energies. JQSRT . 2006 Nov 30;102(2):203-11.. DOI:10.1016/j.jqsrt.2006.02.007.
18. Tekin H.O. MCNP-X Monte Carlo Code Application for Mass Attenuation Coefficients of Concrete at Different Energies by Modeling 3 × 3 Inch NaI(Tl) Detector and Comparison with XCOM and Monte Carlo Data. Science and Technology of Nuclear Installations. 2016 Jul 31;2016. DOI: 10.1155/2016/6547318
19. Akkurt I, Tekin H.O., Mesbahi A. Calculation of Detection Efficiency fort he Gamma Detector using MCNP-X" Acta Physica Polonica A. 2015 Aug 1;128(2):332-4. DOI:10.12693/APhysPolA.128.B-332.
20. Tekin H.O, Kara U. Monte Carlo Simulation for Distance and Absorbed Dose Calculations in a PET-CT Facility by using MCNP-X. Journal of Communication and Computer. 2016; (13): 32-5. DOI:10.17265/1548-7709/2016.01.005
21. Tekin H.O, V. P. Singh, Kara U, Manici T, Altunsoy E.E. Investigation of Nanoparticle Effect on Radiation Shielding Property Using Monte Carlo Method. CBU Journal of Science. 2016;12(2). DOI: 10.18466/cbujos.15586
22. Tekin H.O, Singh V.P, Manici T. An Investigation on Shielding effect of Bismuth on Lung CT Scan using Monte Carlo Simulation. Journal of Polytechnic. 2016; 19 (4): 617-20. DOI:10.2339/2016/19.4.617-622
23. Tekin H.O., Singh V.P., Manici T. Effects of micro-sized and nano-sized WO3 on mass attenuation coefficients of concrete by using MCNP-X code. Applied Radiation and Isotopes. 2016. DOI: 10.1016/j.apradiso.2016.12.040.
24. Tekin H.O, Manici, T. Simulations of mass attenuation coefficients for shielding materials using the MCNP-X code. Nuclear Science and Techniques. 2017;, 28: 95. DOI:10.1007/s41365-017-0253-4
25. Jabbari I, Monadi S. Development and validation of MCNP-X-based Monte Carlo treatment plan verification system. J. Med. Phys. 2015; (40) : 80-9. DOI: 10.4103/0971-6203.158678.
26. E. E. Ermis, F. B. Pilicer, E. Pilicer, C. Celiktas. A comprehensive study for mass attenuation coefficients of different parts of the human body through Monte Carlo methods. Nuclear Science and Techniques. 2016; 27:54. DOI: 10.1007/s41365-016-0053-2.